water

MDPI

Article

Close Association between Stream Water Quality and Fluorescence Properties of Dissolved Organic Matter in Agriculture-Dominated Watersheds

Pilyong Jeon [1], Sohyun Cho [1], Jin Hur [2], Hyunsaing Mun [1], Minhee Chae [1], Yoonhae Cho [1], Kwangseol Seok [1] and Seonhwa Hong [1,*]

[1] Geum River Environment Research Center, National Institute of Environmental Research, 182-18 Jiyong-ro, Okcheon-eup, Okcheon-gun 29027, Korea
[2] Department of Environment and Energy, Sejong University, 209, Neungdong-ro, Gwangjin-gu, Seoul 05006, Korea
* Correspondence: hsh1030@korea.kr

Abstract: The characteristics of dissolved organic matter (DOM) and its relationships with other environmental factors are beneficial for comprehending water pollution in watersheds. This study aimed to improve our understanding of the association of DOM with water quality by connecting the spectroscopic characteristics of DOM with land cover and land use (LCLU). Clustering the tributaries of the Miho upstream watershed according to LCLU resulted in Clusters 1 and 2 having a large proportion of farmland and a large forest area, respectively. Various fluorescence indices derived from fluorescence excitation-emission matrix spectra revealed that livestock effluent resulted in the enrichment of autochthonous organic matter of algal or microbial origin in catchment areas with a high proportion of farmland. Furthermore, to analyze water quality changes according to the land-use characteristics, the water quality and spectroscopic characteristics of DOM were utilized based on the period of farmland use. Further correlation analysis indicated a high correlation between the fluorescence index (FI) in Cluster 1 and organic matter parameters and nitrogenous pollution (Total nitrogen (TN), Dissolved total nitrogen (DTN) and Nitrate nitrogen (NO_3-N)) (planting season, r = 0.991, post-planting season, r = 0.971). This suggests that the FI can be used as a surrogate to estimate the degree of water pollution in watersheds largely affected by land uses related to agricultural activity and the livestock industries.

Keywords: dissolved organic matter; fluorescence index; hierarchical clustering; livestock effluent; active farming

Citation: Jeon, P.; Cho, S.; Hur, J.; Mun, H.; Chae, M.; Cho, Y.; Seok, K.; Hong, S. Close Association between Stream Water Quality and Fluorescence Properties of Dissolved Organic Matter in Agriculture-Dominated Watersheds. *Water* **2022**, *14*, 2459. https://doi.org/10.3390/w14162459

Academic Editor: Ali Saber

Received: 22 June 2022
Accepted: 4 August 2022
Published: 9 August 2022

1. Introduction

Dissolved organic matter (DOM) exists in various aquatic environments, including rivers, lakes, groundwater, and wastewater. It has inhomogeneous structures with a complex mixture, due to bonding with various functional groups such as amide, carboxyl, hydroxyl, and ketone [1]. DOM can be divided by origin into allochthonous and autochthonous DOMs, which have different structural characteristics. On the one hand, allochthonous DOM has non-biodegradable and hydrophobic characteristics because the organic matter in soils is introduced by the mutual exchange between surface- and groundwater or by infiltration or outflow. On the other hand, autochthonous DOM has relatively biodegradable and hydrophilic characteristics because it is generated by algal and microbial activities [2,3]. These DOM types need to be managed because they are known to increase the mobility of pollutants in aquatic environments and negatively affect bioavailability by bonding with heavy metals and hydrophobic organic pollutants [4].

Some DOM exists as fluorescent dissolved organic matter (FDOM) in water and is composed of non-biodegradable matter such as humic and fulvic acids, which are

humic substances, and biodegradable matter such as tryptophan and tyrosine [5]. The origins of DOM components can be inferred using the optical properties of this organic matter [6]. Recently, many studies have been conducted on the classification, origin inference, biochemical reaction mechanism, and pollutant reduction monitoring of DOM and water quality assessment in polluted rivers using the characteristics of FDOM [7–11]. Fluorescence spectroscopy has the advantage of producing results even with a small number of samples and generating much information about DOM in a short time because the measurements in the pretreatment process are performed simply through filtration without using reagents [12]. Fluorescence analysis is a relatively simple method that can obtain a wide range of information about DOM in water, and the fluorescence characteristics of DOM can be analyzed by property [13,14]. Excitation-emission matrix (EEM) analysis enables the interpretation of data in a wide range of excitation and emission wavelengths contained in a fluorescing water sample. Through this process, the mixed fluorescent components of complex DOM in river- and wastewater can be used as "fingerprints" [15,16]. Furthermore, fluorescence indices have been developed to examine the origins and characteristics of DOM [6,17]. Recently, several examples of the use of such fluorescent characteristics and general water quality parameters (e.g., biochemical oxygen demand (BOD), suspended solids (SS), total nitrogen (TN), total phosphorus (TP), pH, NH_3-N) in combination with statistical analysis methods, such as correlation analysis for water quality monitoring, have been reported [18,19]. However, the reported research results are still limited in that the results can only explain the corresponding river watersheds or are only applicable to specific wastewater. Existing literature indicates that the concentration and optical characteristics of DOM are greatly affected by land use, precipitation, and rainfall intensity [20,21]. In particular, intensive land use near rivers and organic pollutants of various origins have been reported to threaten the health of aquatic ecosystems directly and indirectly by greatly deteriorating the water quality of the watershed [15,22,23]. Therefore, it is necessary to explain the correlation between water quality and the fluorescent characteristics of DOM in terms of land use in the watershed.

In this study, the Miho stream watershed was selected for investigation. This watershed is most important for managing water flow and quality for the Geum River, one of the four major rivers of South Korea. Recently, the problem of increasing non-point pollution during rainfall has escalated in the Miho upstream watershed due to an increase in industrial complexes, including food factories, the enlargement and expansion of livestock houses, and the increase in impervious areas. As a result, the health of the river is rapidly degrading [24].

There have been studies reported which predict water quality using the fluorescence properties of the DOM, but they have limitations that are not applicable in various watersheds. Our aim is to diminish limitations and apply water quality prediction using fluorescence analysis. We predict that we will be able to apply the technique to all the various watersheds and be able to easily compare data because fluorescence analysis is an easy and simple method. Therefore, this study aimed to: (1) analyze the correlations of DOM fluorescence data with water quality data and upstream land use in the Miho stream watershed and (2) examine the characteristics and origins of pollutants according to watershed land use. Especially, if the land use of a particular industry is predominant, the correlation between particular fluorescence characteristics and water quality will be high.

2. Materials and Methods

2.1. Study Area and Sampling Sites

The Miho Stream is the first tributary of the Geum River, located in the central region of South Korea, and the upstream watershed of this stream was selected as the study area. Among the tributaries of the Geum River, the Miho stream has the largest watershed area (1855 km^2) and the largest source of pollution to the mainstream. The 10-year (2012–2021) average water quality of BOD, TP and TOC in the Miho Watershed is 4.3 mg/L, 0.14 mg/L, 5.9 mg/L, respectively. According to the Environmental Policy of living waters assessment

in Korea's rivers, there were a significant number of pollutants that was evaluated and determined for use as agricultural water or industrial water after advanced purification treatment [25]. The average temperature in this area is 13.1 °C. The highest monthly average temperature in August is 26.2 °C. In January the average temperature is −1.5 °C and the annual temperature is 27.7 °C. Annual precipitation is 1232.4 mm. In the summer (Jun.–Aug.) the precipitation is 708.0 mm, which accounts for 57.4% of the annual precipitation. In the winter (Dec.–Feb.) the precipitation is 74.7 mm, which accounts for 6.1% of the annual precipitation. The Miho upstream watershed occupies 15.4% (285.3 km^2) of the total watershed area of the Miho stream and the main cultivated plant is rice.

This watershed requires organic matter management because it comprises various land uses, with steadily increasing water consumption for livestock and domestic uses, as well as the release of effluents. Six main tributaries that flow into the Miho upstream watershed were selected as sampling sites (Figure 1). For the land use data of the Miho upstream watershed, the KOMSAT2 image data of 2019 with a 1-m resolution provided by the Ministry of Environment of South Korea were used [26]. Data for livestock, which are regarded as the largest contributor to pollution in the Miho upstream, are collected annually in accordance with Article 23 of the Water Environment Conservation Act. In this study, we analyzed data from 2019 (Table 1). Each of the selected sampling sites, T1–T6, which are tributaries flowing into the Miho upstream, have different characteristics. T1 had the smallest watershed area of 4.7 km^2 and consisted of agricultural, urban, and pasture areas (in descending order of area). Furthermore, T1 had the highest distribution of livestock farms among the sampling sites, with 384 heads/km^2 for cows and 3039 heads/km^2 for pigs (Tables 1 and 2). T3 had the largest watershed area of 34 km^2 among the sampling sites and consisted of agricultural, forest, urban, and pasture areas (in descending order of area). T4 had the second-largest proportion of urban area among the sampling sites, and unlike other sites, there were industrial complexes and wastewater treatment plants servicing industries located near the stream. T6 had the second-highest distribution of pigs (461 heads/km^2), swine manure treatment plants, and village sewage treatment plants among the sampling sites. T5 had the highest proportion of forest area and the lowest distribution of livestock farms (Table 1). The study period was from June 2020 to May 2021, and sampling was performed eight times (June, October, November, and December 2020 and February, March, April, and June 2021). Sampling was performed when there was no effect of rainfall on the sampling sites and when the best water quality characteristics were observed during the sampling month and in each respective month.

Table 1. Number of Livestock in 2019.

Site	Cows	Dairy Cows	Pigs
T1	1807 (384 heads/km^2)	-	14,282 (3039 heads/km^2)
T2	1857 (95 heads/km^2)	-	-
T3	2507 (74 heads/km^2)	61 (2 heads/km^2)	8184 (241 heads/km^2)
T4	875 (38 heads/km^2)	421 (18 heads/km^2)	5468 (240 heads/km^2)
T5	780 (26 heads/km^2)	54 (2 heads/km^2)	1550 (52 heads/km^2)
T6	1059 (74 heads/km^2)	460 (32 heads/km^2)	6596 (461 heads/km^2)
Total	19,635 (69 heads/km^2)	2838 (10 heads/km^2)	121,171 (425 heads/km^2)

Table 2. Land use and land cover of the Miho upstream watershed.

Site	Urban Area (%)	Agricultural Area (%)	Forest Area (%)	Pasture Area (%)	Barren Area (%)	Water Bodies Area (%)	Watershed Area (km^2)
T1	28.14	44.90	4.46	16.26	4.92	1.32	4.7
T2	23.53	41	11.38	16.73	5.22	2.15	19.6
T3	22.67	30.37	23.65	16.81	3.53	2.97	34.0
T4	26.85	25.22	28.50	12.69	3.22	3.52	22.8
T5	14.95	18.86	49.94	10.34	2.77	3.15	29.6
T6	18.83	30.84	32.37	12.58	4.26	1.12	14.3
Total	14.11	34.91	25.79	16.94	5.33	2.92	285.3

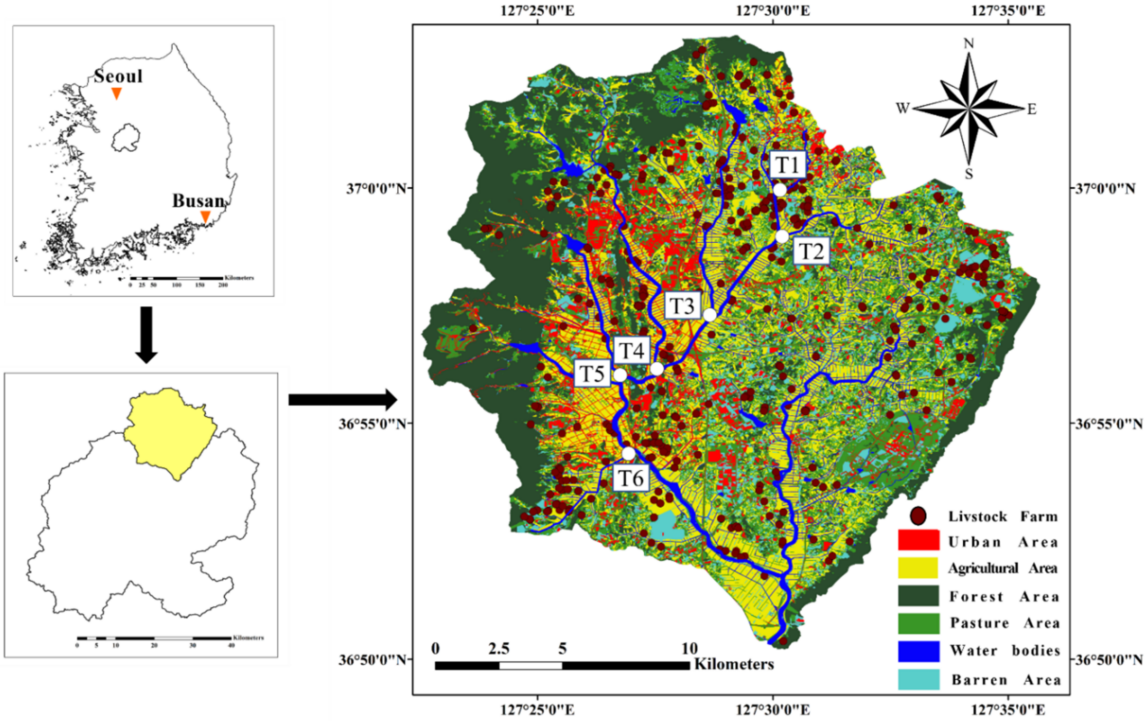

Figure 1. Location of sampling sites in the Miho upstream watershed; white circles indicate the sampling locations (T1: Naetgeureum Stream, T2: Dochung Stream, T3: Sungsan Stream, T4: Chiljang Stream, T5: Guam Stream, T6: Jungsan Stream).

2.2. Flow Rate and Water Quality Measurements

The flow rate was measured during water sampling. To examine the changes in water quality considering the watershed characteristics, sections were divided according to riverbed characteristics at each sampling site and the flow velocity in each section was measured. The flow rate was measured using a current meter (USGS Type AA, USGS Pygmy, Valeport 002; US Geological Survey, Reston, VA, USA), and the flow velocity was calculated by the velocity-area method using the measured flow rate. The flow rate measurement criteria were as follows: distribution of subsection within 5% of the flow rate, minimum measuring time of 40 s, and measurement for more than 120 s at a flow rate of less than 0.2 m/s.

Two litters of sample water were retrieved at the end of the river during every sampling period. For every sample, the electrical conductivity (EC) and dissolved oxygen (DO) were measured immediately on-site using a multiparameter water quality meter (600XL; YSI, Yellow Springs, OH, USA). The collected samples were transported under refrigerated conditions and used in the laboratory for water quality tests for BOD, SS, TN, nitrate nitrogen (NO_3-N), dissolved total nitrogen (DTN), TP, phosphate (PO_4-P), dissolved total phosphorus (DTP), chlorophyll a (Chl-a), total organic carbon (TOC), and dissolved organic carbon (DOC). All parameters were analyzed using standard methods [27].

2.3. Absorbance and Fluorescence Measurements—Fluorescence Spectroscopy and UV Absorbance Analysis

All samples for spectroscopic and fluorescence analyses were filtered using a GF/F filter. The absorbance of each sample was measured at a scanning range of 200–800 nm using a UV-VIS spectrophotometer (Cary Series UV-Vis Spectrophotometer; Agilent Technologies, Santa Clara, CA, USA). The specific UV absorbance (SUVA) is an indicator that indirectly shows aromatic organic carbon compounds using the UV absorption characteristics of DOM. It is calculated by dividing the absorbance at a specific wavelength (254 nm) by the DOC [28]. The spectral slope ($S_{275–295}$) can be determined by the slope of the absorbance

between 275 and 295 nm. $S_{275–295}$ can be used as an indirect predictor of the molecular weight of DOM because it tends to be inversely proportional to the molecular weight [29].

The fluorescence characteristics were analyzed using a fluorescence spectrophotometer (Cary Eclipse Fluorescence Spectrophotometer; Agilent Technologies, Santa Clara, CA, USA). To minimize the effects of light absorbed by the DOM before measuring fluorescence, the sample was diluted using tertiary distilled water so that the absorbance value at 254 nm would be 0.05 or less [14]. The fluorescence intensities of the excitation and emission wavelengths were adjusted using a slit fixed at 10 nm. The samples were measured by adjusting the excitation wavelength range from 200 to 500 nm in 5 nm increments, and the emission wavelength range from 280 to 550 nm in 1 nm increments. The fluorescence intensity can be affected by instrument conditions, such as temperature and humidity. Therefore, to exclude these effects, the fluorescence spectrum of the tertiary distilled water was measured and subtracted. In addition, the values were corrected by normalizing them to an excitation wavelength region of 350 nm or less in the Raman spectrum [30]. The indices of the characteristics and origins of the DOM were calculated using the measured EEM data. Among the calculated indices, the fluorescence index can be used to infer the allochthonous and autochthonous origins of DOM. The biological index is used to indicate the time of formation and the possibility of biodegradability by aquatic microbial activities, while the humidification index indicates the degree of humidification.

2.4. Statistical Analysis

The Shapiro–Wilk normality test was performed to check the normality of the data. Significant differences among the data can be verified by the analysis of variance test for data that show normality and by the Kruskal–Wallis test for non-normal data. The data used in the present study were non-normal according to the Shapiro–Wilk normality test. Thus, the data were analyzed using the Kruskal–Wallis test and the differences among the sampling sites were verified by Dunn's test. To analyze the relationship between fluorescence characteristics and water quality that analyzed the parameters on this study, we used clustering, principal component analyses (PCA), and correlation analyses, which are used as nonparametric methods for analyzing non-normal distributions. Since rice is the main source of cultivation in the area, all of the data was divided into three distinct seasons based on the rice planting season and comparatively analyzed. The first was the pre-planting season (February, March, and April), the second was the planting season (May and June), and the third was the post-harvesting season (October, November, and December). In addition, data normalization was performed so that the characteristics of the data would be equally considered and analyzed. Among the clustering analysis methods, hierarchical clustering analysis (HCA) [31] is widely used. The similarity of data was determined by calculating the Euclidean distance using Ward's method and checked by visualizing it in a dendrogram. The reliability of the correlation analysis results was determined using Spearman's rank correlation coefficient and the *p*-value. The suitability of the data for PCA was evaluated using the KMO (Kaiser–Meyer–Olkin) method, and the principal component number was determined by the eigenvalue [32]. In this study, land use characteristics representing sampling sites were clustered using HCA. Based on the clustering results, the relationships among the parameters (field data (TN, NO_3-N, DTN, TP, PO_4-P, DTP), organic matter parameters, nutrient data, fluorescence, and spectroscopic indices) were examined using Spearman's rank correlation and PCA. All statistical analyses were performed using R software version 4.0.0(R Core Development Team, 2020, Vienna, Austria).

3. Results and Discussion

3.1. Land Use/Cover Similarity and Site Clustering

The characteristics of each land use were distinguished using HCA to examine the effects of Land use and Land cover (LULC) on the watershed. The results were visualized using a dendrogram, and the sampling sites were divided into two clusters based on the similarity of land use (urban, agriculture, forest, pasture, barren, and waterbodies)

(Figure 2). Cluster 1 (C1), which includes T1 and T2, can be interpreted as a watershed area with a high inflow of artificial water pollutants due to livestock, urban and agricultural areas that account for more than 60% of the area. Cluster 2 (C2), which includes T3, T4, T5, and T6, can be considered a watershed area less affected by pollutants due to a large forest area and a small proportion of artificial areas compared with C1.

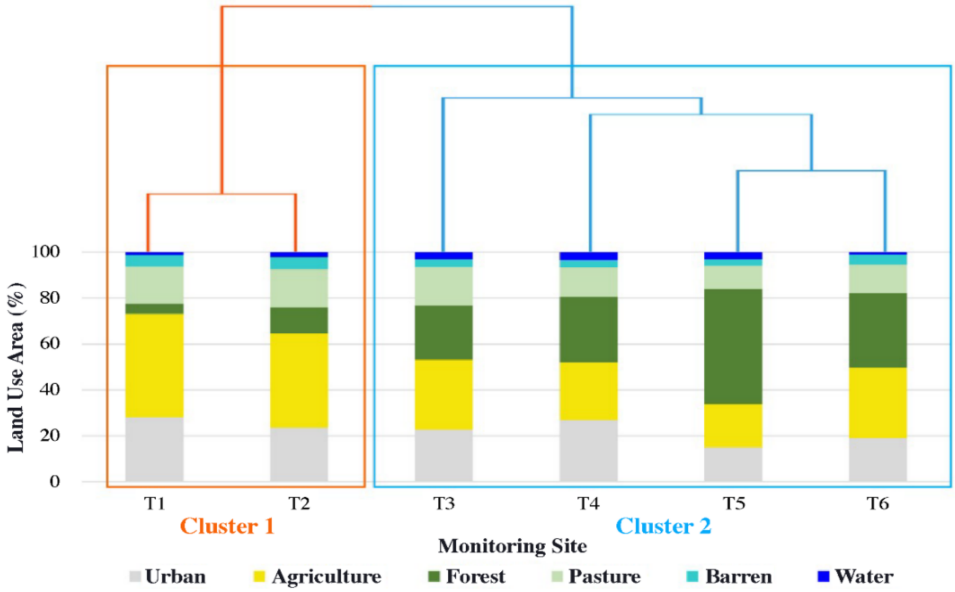

Figure 2. Cluster analysis results according to the characteristics of land use/cover in major tributary basins of the Miho upstream watershed.

3.2. Comparison of Water Quality for Different Tributaries

The monthly data from June 2020 to June 2021 for the six sampling sites were compared separately for field data, organic matter parameters, and nutrient data (Figure 3). The DO, EC, and flow rate values obtained in the field were in the range of 6–16.6 mg/L, 199–1999 μS/cm, and 0.01–0.43 m^3/s, respectively. For both the EC and flow rate, T1 were significantly lower from the other sampling sites. The minimum EC was high at 578 μS/cm, indicating the continuous inflow of considerable amounts of ionic matter ($p < 0.025$). The BOD, TOC, and DOC, which are organic matter parameters, were in the range of 0.6–14.3, 3–31.5, and 2.4–28.6 mg/L, respectively. At T1, the density of the barn is high, so it was affected by livestock wastewater. This is consistent with the result that the inflow of wastewater affects the increase in organic matter concentration in rivers [33]. The averages (±SD) of T1 for BOD, TOC, and DOC were highest at 6.31 (±4.15), 20.96 (±7.73 mg/L), and 17.9 mg/L (±6.56 mg/L), respectively. As for BOD, T4 and T5 showed significant differences from the other sampling sites ($p < 0.025$). Regarding TOC and DOC, T1 showed significant differences from the other sampling sites ($p < 0.025$). The TN, DTN, and NO_3N concentrations, which are nutrient data, ranged from 1.74–53.49, 1.48–52.7, and 0.68–29.74 mg/L, respectively. T1 showed the highest TN, DTN, and NO_3N values at 25.35 mg/L (±11.21), 25.01 (±11.03), and 16.18 mg/L (±6.25 mg/L), respectively, and the differences were significant ($p < 0.025$). TP, DTP, and PO_4P were in the range of 0.05–0.5, 0.04–0.47, and 0.01–0.4 mg/L. T6 showed the highest average TP, DTP, and PO_4P values at0.26 (±0.1), 0.22 (±0.11), and 0.17 mg/L (±0.1 mg/L), respectively, while T4 had relatively low water pollution and showed significant differences compared to other sampling sites ($p < 0.025$). These results revealed differences between sites where water was treated in accordance with the criteria of the sewage treatment plant and sites where the treatment was insufficient. EC has been used together with temperature as a tracer that indicates the behavior and pollution sources of water bodies [34,35]. T1 showed higher organic matter parameters and higher nitrogen pollution than the other sites. Nitrogen fertilizer and livestock wastewater are known to be major sources of nitrogen pollution in agricultural

areas [36,37]. Thus, it can be inferred that T1 has high index values due to the effects of nearby farmlands and livestock pens.

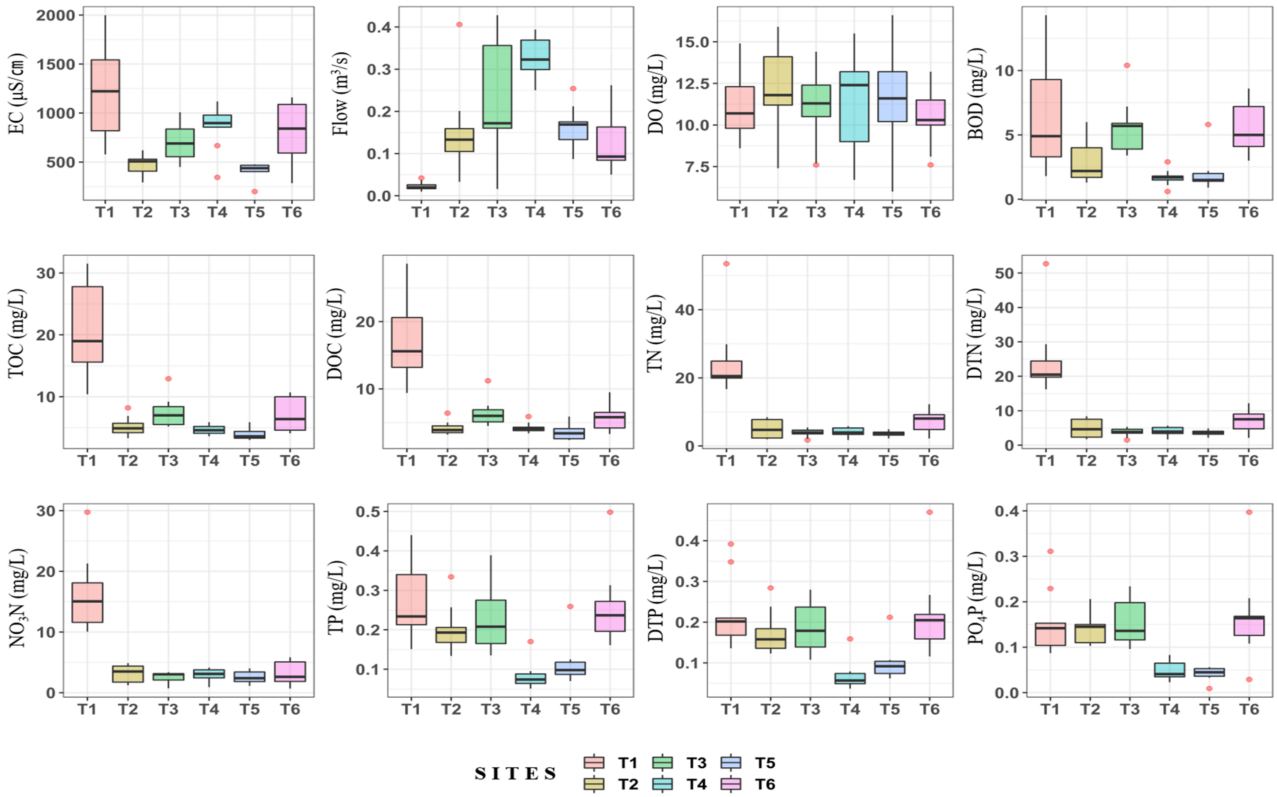

Figure 3. Comparison of field data (EC, flowrate, and DO), organic matter parameters (BOD, TOC, and DOC), and nutrient data (TN, NO_3N, DTN, TP, DTP, and PO_4P) for the six major tributaries of the Miho upstream watershed.

The two clusters were additionally compared based on the farming season, which is a period of artificial activities that are considered to have a significant effect on the water quality characteristics of the watershed (Figure 4). The organic matter and nutrient indices mostly showed higher values in C1 than in C2. In C1, nitrogenous factors tended to be high in the post-harvesting season, and the phosphorous factors tended to be high in the planting season. Phosphorus is known to transport from human-dominated watersheds such as agriculture areas, urban areas, and mixed areas by fertilizers, manure and industrial effluent into rivers [38–40]. In this study, C1 was affected by farming due to the considerable proportion of agricultural areas. The phosphorous factor was high in the planting season due to the direct phosphorous release from the fertilizers used during the planting season. Furthermore, the nitrogenous factors were high in the post-planting season due to the decreased flow rate in the dry season and the considerable impact of base flow post-farming.

3.3. Comparison of Fluorescence and Spectroscopic Indices for Different Tributaries

Along with water quality, fluorescence and spectroscopic indices were similarly compared (Figure 5, Table 3). The fluorescence index (FI), biological index (BIX), humidification index (HIX), specific UV absorbance$_{254}$ ($SUVA_{254}$), and spectral slope ($S_{275–295}$) were in the ranges of 1.43–2.07, 0.62–1.09, 1.59–15.65, 0.52–3.47 L/mg m, and 0.001–0.0019, respectively.

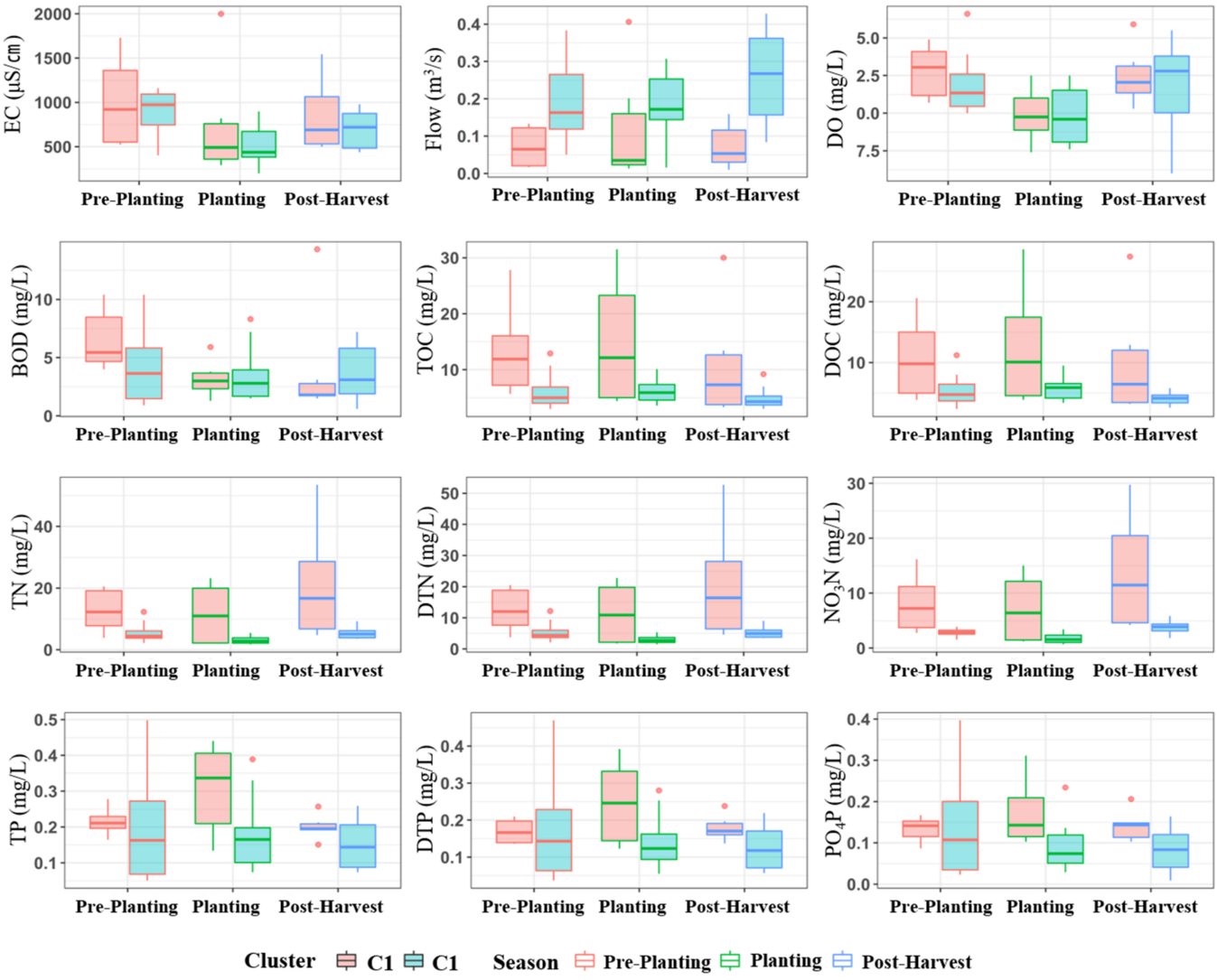

Figure 4. Analysis results for field data, organic matter parameters, and nutrient data according to the two clusters and farming seasons.

When the FI value was smaller than approximately 1.4, allochthonous organic matter from terrestrial sources was dominant. A higher FI value indicated that the autochthonous organic matter of algal or microbial origin, such as secretions from algae and microorganisms, was more dominant [6,41]. The range of FI in the major tributaries of the Miho upstream watershed was 1.43–2.07, and the FI values in most cases were higher than 1.4. Thus, autochthonous organic matter of algal or microbial origin was more dominant than allochthonous organic matter of terrestrial origin. T1 showed the highest average (SD) value of 1.92 (±0.09). A BIX value closer to or larger than 1 indicated that recently generated DOM is dominant. When the BIX value is smaller than 0.6–0.7, the productivity of DOM is low [17,42]. The BIX range was from 0.62–1.09, with T4 showing the highest BIX value of 0.84 (±0.08). In other words, recently generated DOM in the T4 water body was more dominant than in other sampling sites. In T4, wastewater flows from sewage treatment plants and large industrial complexes, and the BIX value was considered high owing to the effect of microorganisms used in the wastewater treatment process. The organic matter in the samples with a HIX value above 10 was predominantly of terrestrial origin and had undergone strong humidification. Conversely, a HIX value less than 4 indicates that the organic matter is derived from plant biomass or animal excrement and is recently generated [43]. The range of HIX in the samples studied was 1.59–15.65, but the HIX values were mostly 10 or lower, except for T1 (11.11 (±2.77)), which indicated a low

DOM of terrestrial origin. Furthermore, a higher $SUVA_{254}$ indicates a higher hydrophobic aromatic organic matter content in the DOM, whereas a lower $SUVA_{254}$ indicates a higher hydrophilic aliphatic organic matter content, which is relatively biodegradable [13]. T1 had the highest $SUVA_{254}$ value of 2.04 (±0.26), indicating a higher concentration of non-biodegradable organic matter than other tributaries. A higher $S_{275–295}$ value indicated lower molecular weights of chromophoric DOM; however, the differences in the average data of the tributaries were not statistically significant. T1 exhibited the highest averages for FI, HIX, and $SUVA_{254}$. In particular, both FI and HIX were high for T1, signifying that DOM of algal or microbial origin and terrestrial origin was high and significantly differed from that of other tributaries ($p < 0.025$).

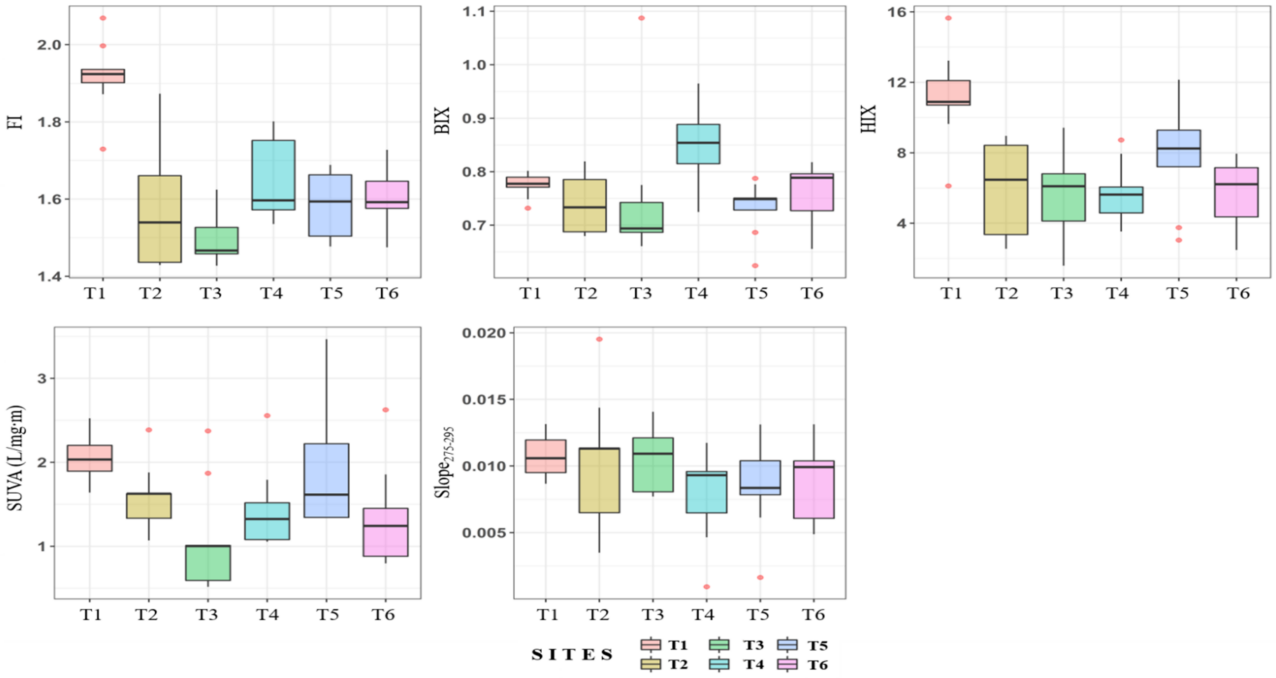

Figure 5. Comparison of fluorescence and spectroscopic indices (FI, HIX, BIX, $SUVA_{254}$, and $Slope_{275–295}$) for the six major tributaries of the Miho stream watershed.

Table 3. Description of fluorescence index properties.

Index	Calculation	Description
Fluorescence index (FI)	$\frac{Em\ 450\ nm}{Em\ 500\ nm}$ *at* $Ex370$ nm	Terrestrial DOM < 1.3–1.4 1.8–1.9 < algal–microbial DOM [6]
Biological index (BIX)	$\frac{Em\ 380\ nm}{Em\ 430\ nm}$ *at* $Ex310$ nm	Less autochthonous DOM < 0.6–0.8 0.8–1.0 < Autochthonous and newly generated sources [17]
Humidification index (HIX)	$\frac{\sum Em\ 435\ nm-480\ nm}{\sum Em\ 300\ nm-345\ nm}$ *at* $Ex254$ nm	Higher HIX indicates increasing humidification [44]

3.4. Understanding of Pollutants Source using Fluorescence and Spectroschpic Characteristics

Among the fluorescence techniques, EEM is among the most convenient analysis methods, and it can provide a different fluorescent matrix to classify various wastewaters and pollutants [5,15]. To examine the fluorescence and spectroscopic indices of T1 in detail, the EEM spectra were compared between T1 and effluent from a nearby swine manure treatment plant in March. The characteristics of pollution sources could be identified best due to a low flow rate, as shown in Figure 6. The EEM spectra were divided into five regions: aromatic protein-like1 (region 1), aromatic protein-like2 (region 2), fulvic acid-like (region 3), soluble microbial by-product-like (SMP, region 4), and humic acid-like (region 5),

according to the method suggested by Chen et al. [45]. The EEM of T1 showed a similar pattern to that of the effluent from the swine manure treatment plant, as the peaks were concentrated in regions 3 and 5. Furthermore, the FI and HIX of T1 were 1.94 and 9.64, respectively, and those of the effluent from the swine manure treatment plant were 1.93 and 12.64, respectively. Thus, both showed high FI and HIX values. It is considered that swine manure wastewater still contains humic acids and SMP even after the treatment process in an individual treatment plant [46], and these affect the fluorescence spectrum of the DOM in effluent and downstream river water [47]. Both the FI and HIX exhibited high values due to fluorescent EEM characteristics.

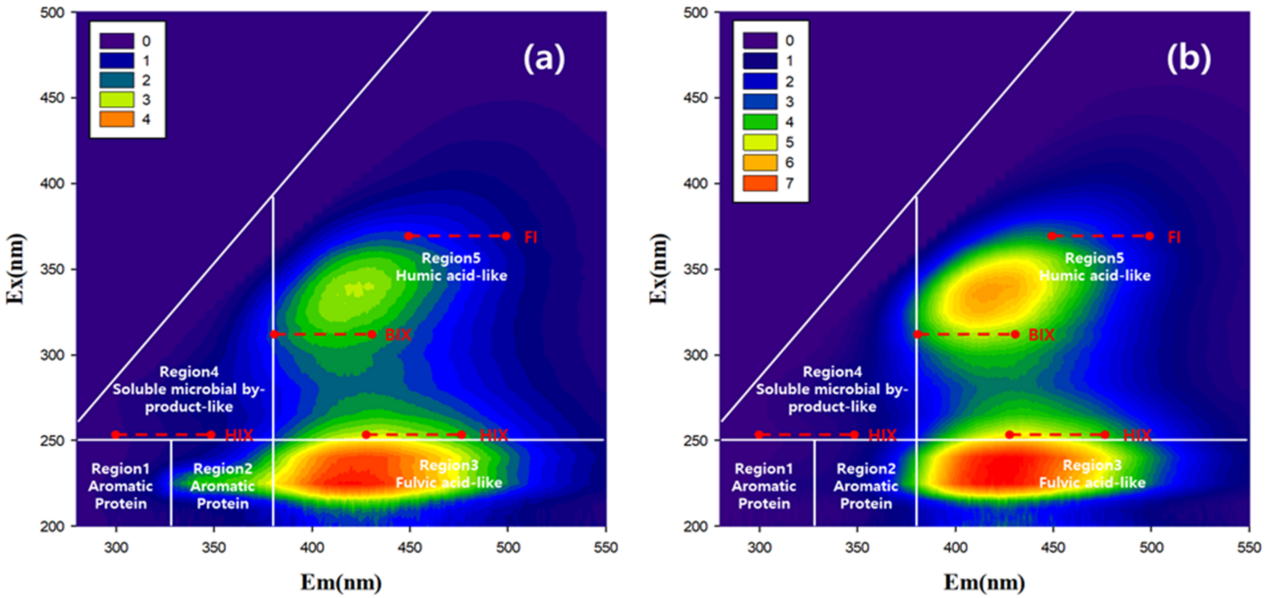

Figure 6. T1 area (**a**) and swine wastewater treatment effluent. (**b**) EEM results and the five regions of EEM based on literature reports [45].

Furthermore, swine manure wastewater effluent displayed a higher SUVA value than other streams because it may contain hydrophobic polymer organic carbon compounds, which are difficult to treat. According to a previous study, the distributions of humic- and fulvic-like components in the EEM of organic matter in cow and swine manure were similar when the cow and swine manure were treated by anaerobic digestion [48]. In particular, the livestock densities of pigs and cows in T1 were much higher than those in other regions at 3039 and 384 heads/km^2, respectively. This suggests that the organic matter in T1 could be affected by cow and swine manure wastewater. These EEM characteristics can be used to track the effects of livestock wastewater in streams.

As with the water quality characteristics, the fluorescence indices were compared between the two clusters divided based on the farming season (Figure 7). Among the fluorescence indices, FI and HIX were higher in C1 than in C2, and this could be attributed to the presence of sampling site T1 in C1. Site T1 was an agricultural area in which livestock farms were scattered with high FI and HIX values. Furthermore, FI and BIX were highest in the pre-planting season and lowest during the planting season in both clusters. This was in contrast to the HIX and $SUVA_{254}$ trends and could be due to the effect of rainfall during the planting season. During rainfall periods, FI tended to decrease, while HIX increased. This may be due to the inflow of organic matter of terrestrial origin carried by rainwater, which decreased the ratio of organic matter of algal or microbial origin [48–50]. $S_{275–295}$ displayed an increasing trend during the planting season, followed by a decrease in the post-harvesting season in C1 and C2. In a recent study, the $S_{275–295}$ value was high in the spring and summer and low in the winter; this trend is similar to that in our study, because it is periodically similar to the farming season classification

used [51]. The $S_{275–295}$ value increased during the planting season because organic matter was decomposed to help with growing plants, resulting in DOM with a relatively low molecular weight becoming dominant.

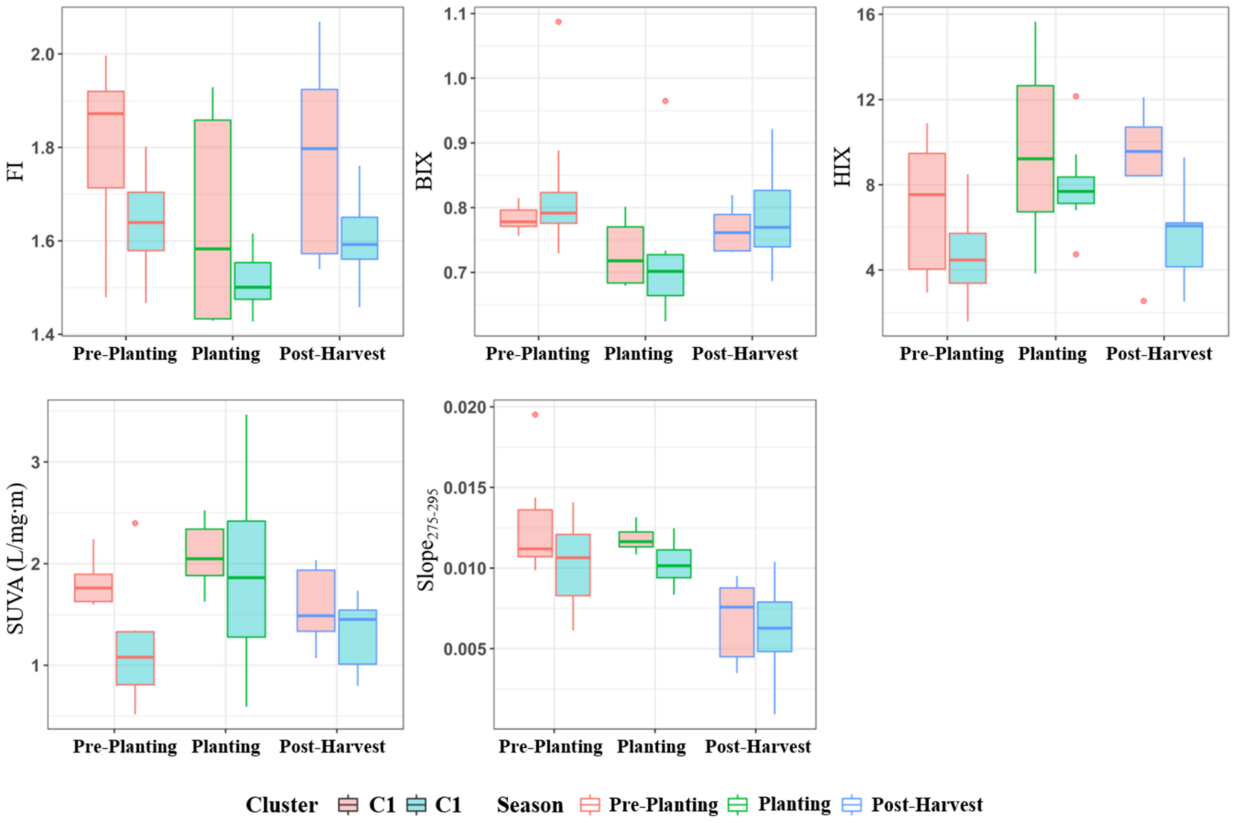

Figure 7. Analysis results for fluorescence and spectroscopic indices according to the two clusters and farming seasons.

3.5. Correlation Analysis between Water Quality Parameters and Spectroscopic Indices for Different Groups According to Land Use and Farming Season

To compare the correlation between the spectroscopic indices of DOM and water quality parameters according to farming season by land-use type, correlation analysis was conducted by cluster and season (Figure 8). The results revealed that there were more parameters with a high correlation between the fluorescence characteristics and water quality parameters in C1 than in C2. C1 consisted of large agricultural areas, and the above results indicated that there was a high correlation between the spectroscopic indices and water quality parameters in such areas. That is, this suggests that dividing clusters by LCLU increases the correlation between the spectroscopic indices and water quality parameters. In C1, FI and HIX showed a high, negative (−0.641 to −0.971) correlation with flow rate during the pre-planting, planting, and post-harvesting seasons. This was because the higher flow rate reduced the effect of swine manure wastewater, which was a source of anthropogenic pollution. However, even in C1, differences in correlations between seasons were observed. For example, during the pre-planting season, the fluorescence indices, such as BIX, FI, and HIX, were not highly correlated (r = 0.371–0.657) with the organic matter concentrations, including BOD, TOC, and DOC, and nitrogenous factors. During the planting season, the correlations (r = 0.600–0.991) increased significantly (Figure 8c,e). Studies in other watersheds, as with C2, did not have a high correlation between nitrogenous factors and fluorescence indices [19,51–53]. This is likely because particulate nitrogen and dissolved inorganic nitrogen contributed a significant portion of TN [53]. However, the correlation with FI was high in large agricultural areas, which attributed to the dominance of dissolved organic nitrogen. In particular, TN, DTN, and NO_3N showed considerably

high correlations with FI in the planting and post-harvesting seasons (r = 0.99 and 0.97, respectively; Figure 8g). Various methods have been used to predict and monitor water quality using fluorescence data [18,19].

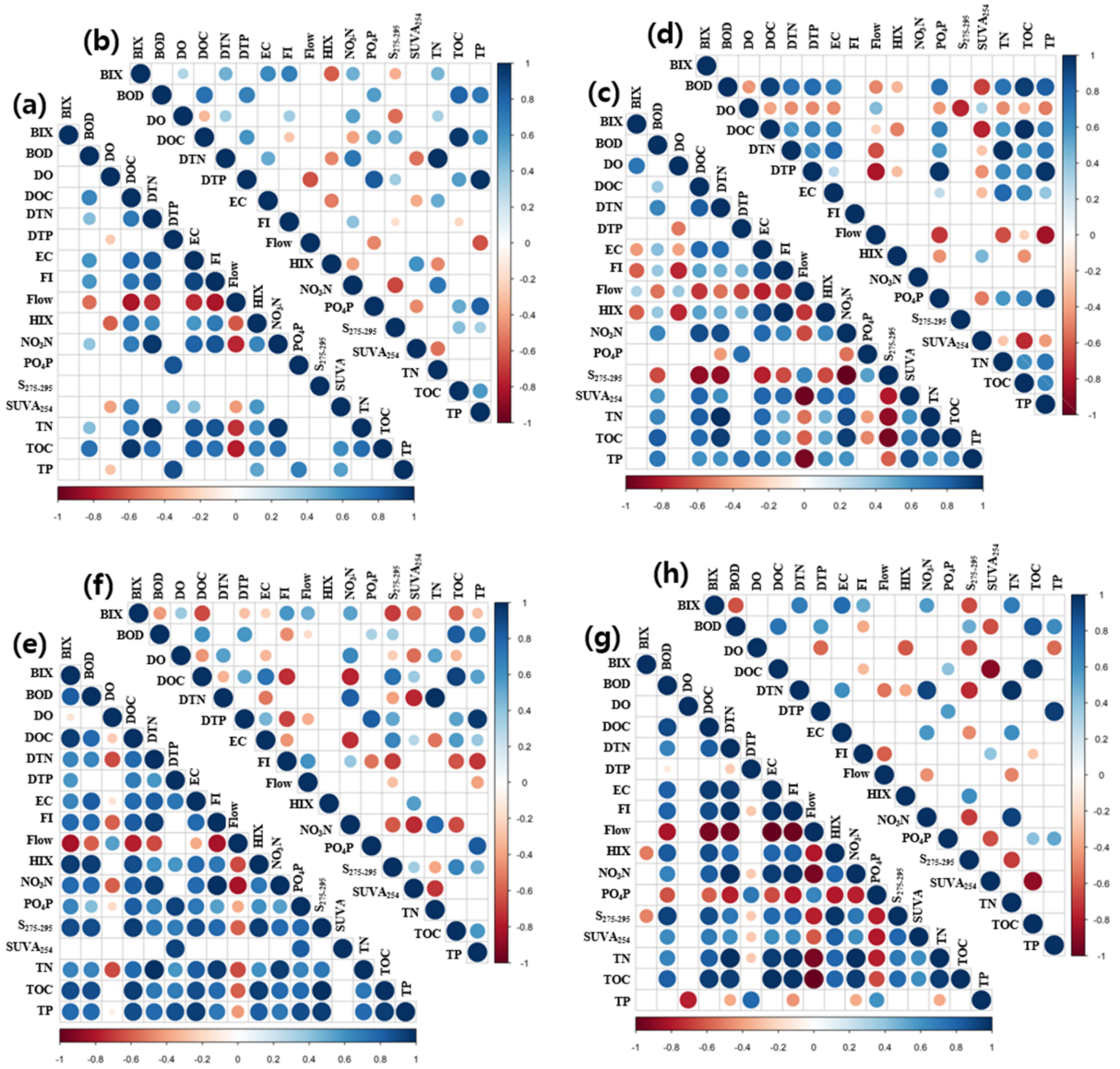

Figure 8. Comparison of correlation coefficients among flow rates, water quality parameters, and spectroscopic indices according to the classified clusters and different farming seasons ($p < 0.01$); all periods, Cluster 1 (C1) (**a**), Cluster 2 (C2) (**b**); pre-planting season, C1 (**c**), C2 (**d**); planting season, C1 (**e**), C2 (**f**); post-harvesting season, C1 (**g**), C2 (**h**).

Therefore, depending on land use, FI can be utilized as an indicator for estimating the degree of nitrogenous organic matter pollution in regions with a large proportion of agricultural area and agricultural activities. A high nitrogen concentration can cause the proliferation of algae and plants, biological diversity reduction, and bad odor [54]. Therefore, estimating the degree of nitrogenous pollution using FI is expected to greatly contribute to determining and predicting aquatic health, as well as water quality monitoring. It was observed that the molecular weight of organic matter increased with increasing DOM concentration in other agricultural watersheds [55,56]. $S_{275–295}$ exhibited high negative correlations (r = −0.657 to −0.991) with BOD, TOC, DOC, EC, and nitrogenous organic pollutants during the pre-planting season in C1 (Figure 8c), but high positive correlations in other seasons (r = 0.714–0.991; Figure 8e,g). This indicates that the molecular weight

of DOM in C1 was proportional to the BOD, TOC, and nitrogenous pollutant contents, and EC during the planting season, but this relationship subsequently became inversely proportional. It appears that DOM with a high molecular weight was decomposed, and its molecular weight decreased in the pre-planting and planting seasons; this was reflected in the concentrations of organic carbon and nitrogenous organic pollutants. This is consistent with the results of $S_{275–295}$, which decreased after agricultural activities, as shown in Figure 7. In C2, where fewer agricultural activities occur, $SUVA_{254}$ was negatively correlated with organic matter parameters, such as BOD, TOC, and DOC, both in the pre- and post-harvesting seasons (Figure 8d,h), suggesting that, as the amount of organic matter in the water decreased, the ratio of non-biodegradable aromatic-carbon-structure organic matter increased. In other words, natural organic matter with a small number of anthropogenic pollutants contains a large amount of non-aromatic biodegradable organic matter.

3.6. Principal Component Analysis Results of the Two Clusters

PCA was conducted to gain a better understanding of the characteristics and meanings of the individual clusters (Figure 9). The PCA results showed that the eigenvalue until the tertiary principal component was 1 or higher in each cluster. In C1, the first and second components accounted for 46.7, 20.3%, respectively, explaining 70% of the total variance (Figure 9a). In C2, the first and second components accounted for 35.9, 24.7%, respectively, explaining 60% of the total variance (Figure 9b). For the first component of C1, the over 0.8 weight factor (EC, TN, DTN, NO_3N, TOC, DOC, FI) can explain the effect on the pollution sources that occur in agricultural and livestock. The second main components of C1 and the first main components of C2, TP, DTP and PO_4P, were shown with a high weight factor of 0.8 or more. This is thought to be due to the characteristics of phosphorus, which is adsorbed or accumulated in soil, unlike nitrogen nutrients and organic matter [57]. In addition, it was derived as the main component due to the effect of sufficient accumulation of phosphorus by cause of manure effluent and fertilizer [58]. It is also judged that phosphorus has been sufficiently accumulated in these watersheds due to livestock manure and fertilizer [58]. FI and HIX, fluorescence indices in C1, were included in the first component's loading as 0.88 and 0.74, respectively, which was consistent with the results of analysis of fluorescence patterns and characterization analysis that watersheds scattered in livestock farms affect FI and HIX.

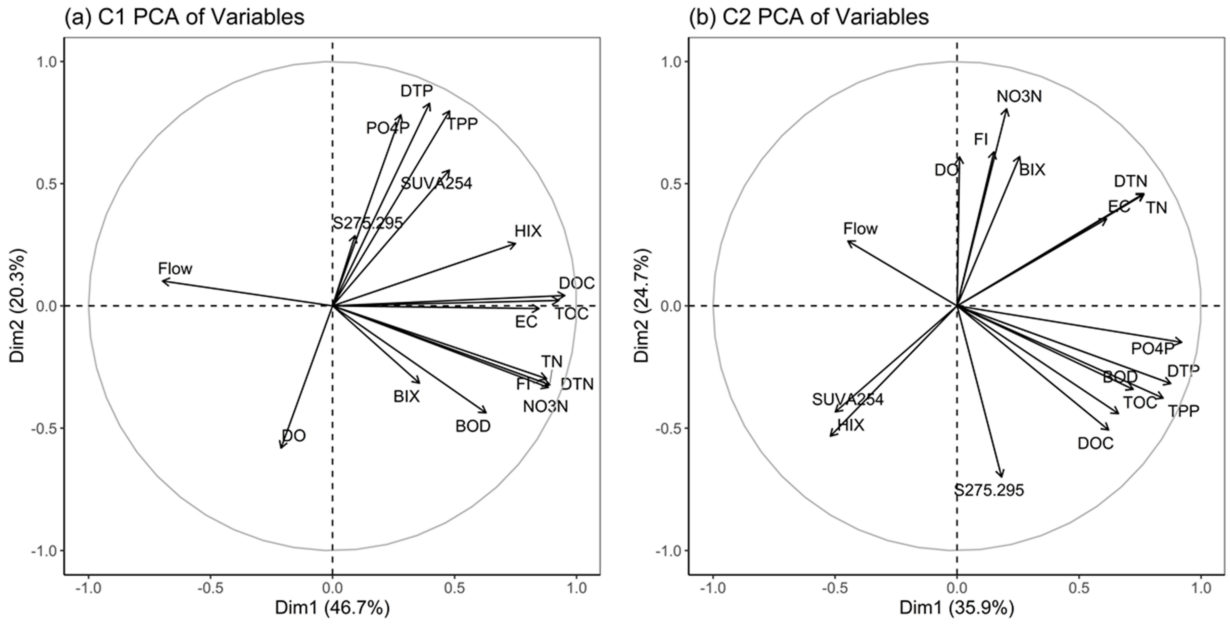

Figure 9. PCA variables of Cluster 1 (**a**) and Cluster 2 sites (**b**).

4. Conclusions

It is crucial to identify organic pollutants and analyze the water pollutant concentrations in watersheds where agricultural and livestock industries and industrial complexes are located. Here, we investigated the land uses and pollutant characteristics of stream watersheds using spectroscopic indices that can be determined rapidly and their correlations with the origins of pollutants. The following conclusions were obtained, along with the results that the correlation between water quality and DOM fluorescence characteristics were high in watersheds with a high ratio of livestock farming and agricultural activities areas.

(1) The stream (T1) where both FI and HIX were high, unlike general streams, was identified, and its EEM fluorescence patterns were analyzed. The fluorescence pattern of T1 was similar to that of the swine manure wastewater treatment plant. The method used in this study can be used in other watersheds to explore the effects of streams polluted by livestock effluent.
(2) On land when using clustering analysis, the Miho upstream watershed was largely divided into watersheds (C1) with much livestock and many agricultural activities and other watersheds (C2). Furthermore, water quality data analysis by the agricultural activity period in each cluster revealed that most water pollution indices were high in areas where livestock farms were located, and the proportion of agricultural area was high.
(3) Analysis of the correlations between fluorescence characteristics and general water quality parameters according to land use clustering revealed that the cluster with a large proportion of agricultural area showed high correlations of fluorescence characteristics and organic matter indices with nitrate ions. This suggests that the degree of nitrogenous and organic matter pollution can be determined using the fluorescence characteristics of watersheds with a large agricultural area proportion (over 40%, in this study). Therefore, it is possible to monitor water quality in various watersheds using clustering and correlation analysis.
(4) The PCA results for C1 and C2 showed that C1 was greatly affected by pollutants due to livestock farming and agricultural activities (the first component). The PCA results for C2 showed that there was less influence of anthropogenic sources than in C1. In addition, the first component of C1, FI and HIX occupied a high weight which confirms that the influence of FDOM was greater in watersheds with a great deal of livestock farming and agricultural activities.

Author Contributions: Conceptualization, P.J. and J.H.; Investigation, P.J., S.C., H.M. and M.C.; Methodology, P.J. and J.H.; Data curation, P.J. and S.C.; Writing-original draft, P.J.; Visualization, S.C.; Software, S.C.; Writing-review and editing, S.C. and S.H.; Supervision, J.H., H.M. and K.S. Funding acquisition, H.M. and S.H.; Validation, M.C. and Y.C.; Formal Analysis, Y.C.; Resource, K.S.; Project administration, S.H. All authors have read and agreed to the published version of the manuscript.

Funding: This research was funded by the Korea Ministry of Environment as the National Institute of Environmental Research, grant number NIER-2021-01-01-026.

Institutional Review Board Statement: Not applicable.

Informed Consent Statement: Not applicable.

Data Availability Statement: The datasets generated and/or analysed during the current study are available from the corresponding author on reasonable request.

Conflicts of Interest: The authors declare no conflict of interest.

References

1. Hur, J.; Lee, B.M.; Shin, H.S. Microbial degradation of dissolved organic matter (DOM) and its influence on phenanthrene-DOM interactions. *Chemosphere* **2011**, *85*, 1360–1367. [CrossRef] [PubMed]
2. Gondar, D.; Thacker, S.A.; Tipping, E.; Baker, A. Functional variability of dissolved organic matter from the surface water of a productive lake. *Water Res.* **2008**, *42*, 81–90. [CrossRef]

3. Leloup, M.; Nicolau, R.; Pallier, V.; Yéprémian, C.; Feuillade-Cathalifaud, G. Organic matter produced by algae and cyanobacteria: Quantitative and qualitative characterization. *J. Environ. Sci.* **2013**, *25*, 1089–1097. [CrossRef]
4. Lee, Y.K.; Hur, J. Using two-dimensional correlation size exclusion chromatography (2D-CoSEC) to explore the size-dependent heterogeneity of humic substances for copper binding. *Environ. Pollut.* **2017**, *227*, 490–497. [CrossRef] [PubMed]
5. Hudson, P.K.; Gibson, E.R.; Young, M.A.; Kleiber, P.D.; Grassian, V.H. A newly designed and constructed instrument for coupled infrared extinction and size distribution measurements of aerosols. *Aerosol Sci. Technol.* **2007**, *41*, 701–710. [CrossRef]
6. McKnight, D.M.; Boyer, E.W.; Westerhoff, P.K.; Doran, P.T.; Kulbe, T.; Andersen, D. Spectrofluorometric characterization of dissolved organic matter for indication of precursor organic material and aromaticity. *Limnol. Oceanogr.* **2001**, *46*, 38–48. [CrossRef]
7. Chen, M.; Price, R.M.; Yamashita, Y.; Jaffé, R. Comparative study of dissolved organic matter from groundwater and surface water in the Florida coastal Everglades using multi-dimensional spectrofluorometry combined with multivariate statistics. *Appl. Geochem.* **2010**, *25*, 872–880. [CrossRef]
8. Hoppe-Jones, C.; Dickenson, E.R.; Drewes, J.E. The role of microbial adaptation and biodegradable dissolved organic carbon on the attenuation of trace organic chemicals during groundwater recharge. *Sci. Total Environ.* **2012**, *437*, 137–144. [CrossRef]
9. McDowell, W.H.; Zsolnay, A.; Aitkenhead-Peterson, J.A.; Gregorich, E.G.; Jones, D.L.; Jödemann, D.; Kalbitz, K.; Marschner, B.; Schwesig, D. A comparison of methods to determine the biodegradable dissolved organic carbon from different terrestrial sources. *Soil Biol. Biochem.* **2006**, *38*, 1933–1942. [CrossRef]
10. Mermillod-Blondin, F.; Simon, L.; Maazouzi, C.; Foulquier, A.; Delolme, C.; Marmonier, P. Dynamics of dissolved organic carbon (DOC) through stormwater basins designed for groundwater recharge in urban area: Assessment of retention efficiency. *Water Res.* **2015**, *81*, 27–37. [CrossRef]
11. Liu, W.X.; He, W.; Wu, J.Y.; Wu, W.J.; Xu, F.L. Effects of fluorescent dissolved organic matters (FDOMs) on perfluoroalkyl acids (PFAAs) in lake and river water. *Sci. Total Environ.* **2019**, *666*, 598–607. [CrossRef]
12. Kalbitz, K.; Schmerwitz, J.; Schwesig, D.; Matzner, E. Biodegradation of soil-derived dissolved organic matter as related to its properties. *Geoderma.* **2003**, *113*, 273–291. [CrossRef]
13. Leenheer, J.A.; Croué, J.-P. Peer reviewed: Characterizing aquatic dissolved organic matter. *Environ. Sci. Technol.* **2003**, *37*, 18A–26A. [CrossRef]
14. Baker, A. Fluorescence excitation− emission matrix characterization of some sewage-impacted rivers. *Environ. Sci. Technol.* **2001**, *35*, 948–953. [CrossRef]
15. Henderson, R.K.; Baker, A.; Murphy, K.R.; Hambly, A.; Stuetz, R.M.; Khan, S.J. Fluorescence as a potential monitoring tool for recycled water systems: A review. *Water Res.* **2009**, *43*, 863–881. [CrossRef]
16. Peiris, R.H.; Budman, H.; Moresoli, C.; Legge, R.L. Identification of humic acid-like and fulvic acid-like natural organic matter in river water using fluorescence spectroscopy. *Water Sci. Technol.* **2011**, *63*, 2427–2433. [CrossRef]
17. Henderson, R.K.; Baker, A.; Murphy, K.R.; Hambly, A.; Stuetz, R.M.; Khan, S.J. Properties of fluorescent dissolved organic matter in the Gironde Estuary. *Org. Geochem.* **2009**, *40*, 706–719.
18. Zhang, X.; Li, B.; Deng, J.; Qin, B.; Wells, M.; Tefsen, B. Regional-scale investigation of dissolved organic matter and lead binding in a large impacted lake with a focus on environmental risk assessment. *Water Res.* **2020**, *172*, 115478. [CrossRef]
19. Zhao, Y.; Song, K.; Wen, Z.; Fang, C.; Shang, Y.; Lv, L. Evaluation of CDOM sources and their links with water quality in the lakes of Northeast China using fluorescence spectroscopy. *J. Hydrol.* **2017**, *550*, 80–91. [CrossRef]
20. Bernal, S.; Butturini, A.; Sabater, F. Variability of DOC and nitrate responses to storms in a small Mediterranean forested catchment. *Hydrol. Earth Syst. Sci.* **2002**, *6*, 1031–1041. [CrossRef]
21. Molinero, J.; Burke, R.A. Effects of land use on dissolved organic matter biogeochemistry in piedmont headwater streams of the Southeastern United States. *Hydrobiologia* **2009**, *635*, 289–308. [CrossRef]
22. Cohen, E.; Levy, G.J.; Borisover, M. Fluorescent components of organic matter in wastewater: Efficacy and selectivity of the water treatment. *Water Res.* **2014**, *55*, 323–334. [CrossRef]
23. Zhao, Y.; Song, K.; Li, S.; Ma, J.; Wen, Z. Characterization of CDOM from urban waters in Northern-Northeastern China using excitation-emission matrix fluorescence and parallel factor analysis. *Environ. Sci. Pollut. Res. Int.* **2016**, *23*, 15381–15394. [CrossRef]
24. Hur, J.W.; Kim, K.H.; Lee, J.J. Calculation (Computation) of Habitat Suitability Index for Swimming Fish Species Living in Miho Stream in Geum River Water System. *Ecol. Resilient Infrastruct.* **2021**, *8*, 9–21.
25. ME, Framework Act on Environmental Policy in Korea. 2020. Available online: https://law.go.kr (accessed on 25 March 2022).
26. ME, Environmental Geographic Information Service(EGIS). 2020. Available online: https://egis.me.go.kr/main.do (accessed on 13 November 2020).
27. Hur, M.; Lee, I.; Tak, B.M.; Lee, H.J.; Yu, J.J.; Cheon, S.U.; Kim, B.S. Temporal shifts in cyanobacterial communities at different sites on the Nakdong River in Korea. *Water Res.* **2013**, *47*, 6973–6982. [CrossRef] [PubMed]
28. Weishaar, J.L.; Aiken, G.R.; Bergamaschi, B.A.; Fram, M.S.; Fujii, R.; Mopper, K. Evaluation of specific ultraviolet absorbance as an indicator of the chemical composition and reactivity of dissolved organic carbon. *Environ. Sci. Technol.* **2003**, *37*, 4702–4708. [CrossRef] [PubMed]
29. Helms, J.R.; Stubbins, A.; Ritchie, J.D.; Minor, E.C.; Kieber, D.J.; Mopper, K. Erratum: Absorption spectral slopes and slope ratios as indicators of molecular weight, source, and photobleaching of chromophoric dissolved organic matter. *Limnol. Oceanogr.* **2009**, *54*, 1023.

30. Søndergaard, M.; Stedmon, C.A.; Borch, N.H. Fate of terrigenous dissolved organic matter (DOM) in estuaries: Aggregation and bioavailability. *Ophelia* **2003**, *57*, 161–176. [CrossRef]
31. Liu, J.; Zhang, D.; Tang, Q.; Xu, H.; Huang, S.; Shang, D.; Liu, R. Water quality assessment and source identification of the Shuangji River (China) using multivariate statistical methods. *PLoS ONE* **2021**, *16*, e0245525. [CrossRef]
32. de Andrade Costa, D.; Soares de Azevedo, J.P.; Dos Santos, M.A.; dos Santos Facchetti Vinhaes Assumpção, R. Water quality assessment based on multivariate statistics and water quality index of a strategic river in the Brazilian Atlantic Forest. *Sci. Rep.* **2020**, *10*, 22038. [CrossRef]
33. Singh, S.; Dutta, S.; Inamdar, S. Land application of poultry manure and its influence on spectrofluorometric characteristics of dissolved organic matter. *Agric. Ecosyst. Environ.* **2014**, *193*, 25–36. [CrossRef]
34. Cirpka, O.A.; Fienen, M.N.; Hofer, M.; Hoehn, E.; Tessarini, A.; Kipfer, R.; Kitanidis, P.K. Analyzing bank filtration by deconvoluting time series of electric conductivity. *Ground Water* **2007**, *45*, 318–328. [CrossRef]
35. Vogt, T.; Hoehn, E.; Schneider, P.; Freund, A.; Schirmer, M.; Cirpka, O.A. Fluctuations of electrical conductivity as a natural tracer for bank filtration in a losing stream. *Adv. Water Res.* **2010**, *33*, 1296–1308. [CrossRef]
36. Lazcano, C.; Zhu-Barker, X.; Decock, C. Effects of Organic Fertilizers on the Soil Microorganisms Responsible for N2O Emissions: A Review. *Microorganisms* **2021**, *9*, 983. [CrossRef]
37. Torres-Martínez, J.A.; Mora, A.; Mahlknecht, J.; Daesslé, L.W.; Cervantes-Avilés, P.A.; Ledesma-Ruiz, R. Estimation of nitrate pollution sources and transformations in groundwater of an intensive livestock-agricultural area (Comarca Lagunera), combining major ions, stable isotopes and MixSIAR model. *Environ. Pollut.* **2021**, *269*, 115445. [CrossRef]
38. Duan, S.; Banger, K.; Toor, G.S. Evidence of phosphate mining and Agriculture influence on Concentrations, forms, and ratios of nitrogen and phosphorus in a Florida River. *Water* **2021**, *13*, 1064. [CrossRef]
39. Boyer, E.W.; Goodale, C.L.; Jaworski, N.A.; Howarth, R.W. Anthropogenic nitrogen sources and relationships to riverine nitrogen export in the northeastern USA. *Biogeochemistry* **2002**, *57*, 137–169. [CrossRef]
40. Russell, M.J.; Weller, D.E.; Jordan, T.E.; Sigwart, K.J.; Sullivan, K.J. Net anthropogenic phosphorus inputs: Spatial and temporal variability in the Chesapeake Bay region. *Biogeochemistry* **2008**, *88*, 285–304. [CrossRef]
41. Cory, R.M.; McKnight, D.M. Fluorescence spectroscopy reveals ubiquitous presence of oxidized and reduced quinones in dissolved organic matter. *Environ. Sci. Technol.* **2005**, *39*, 8142–8149. [CrossRef]
42. Parlanti, E.; Wörz, K.; Geoffroy, L.; Lamotte, M. Dissolved organic matter fluorescence spectroscopy as a tool to estimate biological activity in a coastal zone submitted to anthropogenic inputs. *Org. Geochem.* **2000**, *31*, 1765–1781. [CrossRef]
43. Birdwell, J.E.; Engel, A.S. Characterization of dissolved organic matter in cave and spring waters using UV–Vis absorbance and fluorescence spectroscopy. *Org. Geochem.* **2010**, *41*, 270–280. [CrossRef]
44. Zsolnay, A.; Baigar, E.; Jimenez, M.; Steinweg, B.; Saccomandi, F. Differentiating with fluorescence spectroscopy the sources of dissolved organic matter in soils subjected to drying. *Chemosphere* **1999**, *38*, 45–50. [CrossRef]
45. Chen, W.; Westerhoff, P.; Leenheer, J.A.; Booksh, K. Fluorescence excitation—Emission matrix regional integration to quantify spectra for dissolved organic matter. *Environ. Sci. Techonl.* **2003**, *37*, 5701–5710. [CrossRef] [PubMed]
46. Zeng, Z.; Zheng, P.; Ding, A.; Zhang, M.; Abbas, G.; Li, W. Source analysis of organic matter in swine wastewater after anaerobic digestion with EEM-PARAFAC. *Envrion. Sci. Pollut. Res. Int.* **2017**, *24*, 6770–6778. [CrossRef]
47. Du, X.; Gu, L.P.; Wang, T.T.; Kou, H.J.; Sun, Y. The relationship between the molecular composition of dissolved organic matter and bioavailability of digestate during anaerobic digestion process: Characteristics, transformation and the key molecular interval. *Bioresour. Technol.* **2021**, *342*, 125958. [CrossRef]
48. Saraceno, J.F.; Pellerin, B.A.; Downing, B.D.; Boss, E.; Bachand, P.A.; Bergamaschi, B.A. High-frequency in situ optical measurements during a storm event: Assessing relationships between dissolved organic matter, sediment concentrations, and hydrologic processes. *J. Geophys. Res.* **2009**, *114*, G4. [CrossRef]
49. Nguyen, H.V.-M.; Hur, J.; Shin, H.-S. Changes in Spectroscopic and Molecular Weight Characteristics of Dissolved Organic Matter in a River During a Storm Event. *Water Air Soil Pollut.* **2010**, *212*, 395–406. [CrossRef]
50. Nguyen, H.V.M.; Lee, M.H.; Hur, J.; Schlautman, M.A. Variations in spectroscopic characteristics and disinfection byproduct formation potentials of dissolved organic matter for two contrasting storm events. *J. Hydrol.* **2013**, *481*, 132–142. [CrossRef]
51. Han, Z.; Xiao, M.; Yue, F.; Yi, Y.; Mostofa, K.M.G. Seasonal Variations of Dissolved Organic Matter by Fluorescent Analysis in a Typical River Catchment in Northern China. *Water* **2021**, *13*, 494. [CrossRef]
52. Wang, X.; Zhang, F.; Ghulam, A.; Trumbo, A.L.; Yang, J.; Ren, Y.; Jing, Y. Evaluation and estimation of surface water quality in an arid region based on EEM-PARAFAC and 3D fluorescence spectral index: A case study of the Ebinur Lake Watershed, China. *Catena* **2017**, *155*, 62–74. [CrossRef]
53. Tang, J.; Li, X.; Cao, C.; Lin, M.; Qiu, Q.; Xu, Y.; Ren, Y. Compositional variety of dissolved organic matter and its correlation with water quality in peri-urban and urban river watersheds. *Ecol. Indic.* **2019**, *104*, 459–469. [CrossRef]
54. Mouri, G.; Takizawa, S.; Oki, T. Spatial and temporal variation in nutrient parameters in stream water in a rural-urban catchment, Shikoku, Japan: Effects of land cover and human impact. *J. Environ. Manag.* **2011**, *92*, 1837–1848. [CrossRef]
55. Dalzell, B.J.; King, J.Y.; Mulla, D.J.; Finlay, J.C.; Sands, G.R. Influence of subsurface drainage on quantity and quality of dissolved organic matter export from agricultural landscapes. *J. Geophys. Res. Biogeosciences* **2011**, *116*. [CrossRef]

56. Hernes, P.J.; Spencer, R.G.; Dyda, R.Y.; Pellerin, B.A.; Bachand, P.A.; Bergamaschi, B.A. DOM composition in an agricultural watershed: Assessing patterns and variability in the context of spatial scales. *Geochim. Cosmochim. Acta* **2013**, *121*, 599–610. [CrossRef]
57. Zeng, F.; Zuo, Z.; Mo, J.; Chen, C.; Yang, X.; Wang, J.; Wang, Y.; Zhao, Z.; Chen, T.; Li, Y.; et al. Runoff Losses in Nitrogen and Phosphorus From Paddy and Maize Cropping System: A Field Study in Dongjiang Basin, South China. *Front. Plant Sci.* **2021**, *12*, 1593. [CrossRef]
58. Cui, N.; Cai, M.; Zhang, X.; Abdelhafez, A.A.; Zhou, L.; Sun, H.; Chen, G.; Zou, G.; Zhou, S. Runoff loss of nitrogen and phosphorus from a rice paddy field in the east of China: Effect of long-term chemical N fertilizer and organic manure applications. *Glob. Ecol. Conserv.* **2020**, *22*, e01011. [CrossRef]